Design of Digital Linear-Phase FIR Crossover Systems for Loudspeakers by the Method of Vector Space Projections

Khalil C. Haddad, Henry Stark, *Fellow, IEEE*, and Nikolas P. Galatsanos, *Senior Member, IEEE*

***Abstract*—A new technique for designing digital linear-phase FIR crossover systems for loudspeakers is proposed. The approach is based on the principle of vector space projections. We describe the constraint sets and their projections that capture the properties of the desired crossover filters. The proposed approach is capable of designing crossover networks for multiple band-splitting as well as for equalization. Designs that demonstrate the advantages and flexibility of this method are furnished.**

***Index Terms*— Crossover systems, digital filter design, digital filters, equalization, FIR filters, linear phase, loudspeakers, vector-space projections.**

I. Introduction

CROSSOVER networks are used in loudspeaker systems [1], [2]. Since it is difficult to design a single loudspeaker driver that accurately reproduces all audio frequencies, a high-quality loudspeaker must have two or more drivers (see Fig. 1), where each is specifically designed to operate over a portion of the audio spectrum. The function of a crossover network is to split the audio signal into adjacent frequency bands that are appropriate for each driver. Typically, crossover systems are composed of a parallel combination of filters called *analysis* filters. The frequency in the transition bands at which the filter gain equals that of an adjacent filter is called the *crossover* frequency. The sum of the filter response functions should be relatively constant everywhere, including the transition bands. If this is not the case, irregularities such as peaks and dips in the crossover transition band are heard as undesirable colorings in the sound production.

It is very desirable, among other things, to have an overall loudspeaker/crossover system that produces a flat *sound pressure level* (SPL) near the listener for the entire audio spectrum i.e., without amplitude and phase distortion. However, loudspeakers are passive electromechanical devices that, unfortunately, due to their particular physical and electrical characteristics, introduce errors in amplitude, phase, and crossover characteristics. Traditionally, engineers compensated for these errors by designing crossover systems using analog circuitry. Analog designs can only partially reduce these errors since the filters themselves also introduce some nonlinearities. At the present time, some manufacturers are introducing a digital stage in their design based on DSP or VLSI chips. Equalizers and crossover systems based on FIR and IIR filters are being implemented especially in high-end loudspeaker systems. Digital systems can outperform their analog counterparts in the quality of sound produced since they can be programmed to perform at the level where the distortions caused by loudspeakers are significantly reduced.

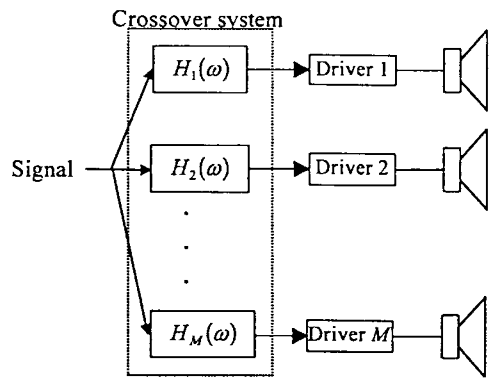

Fig. 1. M-way crossover/loudspeaker system.

Digital crossover networks are capable of splitting the signal into multiple frequency bands and compensate for amplitude distortion without introducing undesirable amplification or attenuation in the crossover bands. It is desirable that they enjoy linear phase response (no phase distortion) and minimal overlap between bands. Moreover, using digital allpass IIR or FIR filters can negate excess phase distortion.

II. Digital Crossover System Characteristics and Design

Consider first the case where the loudspeaker characteristics are ideal (i.e., flat SPL across the entire audio spectrum). In that case, an ideal crossover network will provide the following:

1) a combined linear phase and flat, say, unit magnitude frequency response over the whole band i.e.,

$$H(\omega) = \sum_{i=1}^{M} |H_i(\omega)| e^{j\varphi_i(\omega)} = e^{j\varphi(\omega)} \quad \text{for} \quad 0 \le \omega \le \pi \tag{1}$$

Manuscript received June 8, 1998; revised May 10, 1999. The associate editor coordinating the review of this paper and approving it for publication was Dr. Mahmood R. Azimi-Sadjadi.

K. C. Haddad was with 3Com, Rolling Meadows, IL 60008 USA. He is now with Lucent Technologies, Holmdel, NJ 07733 USA.

H. Stark and N. P. Galatsanos are with the Department of Electrical and Computer Engineering, Illinois Institute of Technology, Chicago, IL 60616-3793.

Publisher Item Identifier S 1053-587X(99)08296-3.

where each $H_i(\omega)$ is the transfer function of the crossover network, and $\varphi(\omega) = \varphi_i(\omega) = \omega(L-1)/2$ for $i = 1, \cdots, M$, where L is the length of each of the M individual filters;

2) adequate steep cut-off rates of the individual filters $H_i(\omega)$;
3) good stopband attenuation for each filter $H_i(\omega)$ to prevent out of band signals from saturating and possibly damaging the speakers.

The filter $H(\omega)$ synthesized from $H_i(\omega)$, as described in (1), defines an element of the class of strictly complementary (SC) filters. If we split a time-discrete signal $x(n)$ into M subband signals using the analysis filters $H_i(\omega)$, then we can add the subband signals to get back a delayed replica of the original signal $x(n)$ with no distortion. When $M = 2$, the design an SC pair can be done as follows: Let $h_1(n)$ be the response of a linear-phase, lowpass filter of an odd length L. Then, $h_2(n) = \delta(n-(L-1)/2) - h_1(n)$ is a highpass filter and is strictly complementary to $h_1(n)$. For an arbitrary M, there exists a subclass of filters known as Mth-band filters or Nyquist (M) filters. For a fixed M, the impulse response $h(n)$ of such filters satisfies

$$h(Mn) = \begin{cases} c, & n = 0 \\ 0, & \text{otherwise.} \end{cases} \tag{2}$$

In other words, $h(n)$ is zero at multiples of M. It can be shown [3] that if $h(n) \leftrightarrow H(\omega)$ with linear phase, then

$$\begin{aligned} F(\omega) &= \sum_{i=0}^{M-1} |H(\omega - 2\pi i/M)| e^{j([L-1]/2)\omega)} \\ &= Mce^{j([L-1]/2)\omega} = e^{j([L-1]/2)\omega} \\ &\qquad (\text{assuming } c = 1/M). \end{aligned} \tag{3}$$

In words, $F(\omega)$ is a multiband, linear-phase filter composed of M uniformly SC analysis filters, which are frequency-shifted versions of $H(\omega)$ with a magnitude that adds up to a constant. A disadvantage in using Mth-band filters as a crossover system is that all the passbands are equal, which is usually inappropriate for the spectrum range of different types of speakers (woofer, mid-range, and tweeter). To be able to design a crossover system with *unequal frequency bands*, a second level of a crossover filters will split a signal into two or more Nyquist subbands. This technique allows a limited choice of crossover frequencies at the expense of increasing additional passband regions.

When the loudspeaker characteristics are not ideal, then a crossover system should also incorporate equalization to correct the speaker SPL aberration in addition to the above characteristics, i.e.,

$$|H(\omega)| = \frac{1}{L(\omega)} \quad \text{for} \quad 0 \le \omega \le \pi \tag{4}$$

where $L(\omega)$ represents the speaker SPL as a function of frequency. The Mth-band filters cannot easily be designed to compensate for the prescribed aberrations. The best we can do is to design a multilevel filter as

$$F(\omega) = \sum_{i=0}^{M-1} \alpha_i |H(\omega - 2\pi i/M)| e^{(j([L-1]/2)\omega)} \tag{5}$$

where α_i represents the level of each band. This may not yield satisfactory equalization.

The disadvantages of crossover filter design by existing methods can be overcome by design based on vector space projections. We review the principles of this technique below.

III. VSPM Background

The *vector space projection method* (VSPM) deals with the problem of finding a mathematical object (for example, a signal, function, image, etc.) in a proper vector space that satisfies multiple constraints. When all the constraint sets are convex and have a *nonempty intersection*, there exists a powerful theory in finding the object that satisfies all the constraints. This subset of VSPM is called *projection onto convex sets* (POCS), which we describe below.

The theory of convex projections, developed by Bregman [4] and Gubin *et al.* [5], was first applied to image processing by Youla and Webb [6]. See [7] for a basic introduction to this method. Additional introductory material and applications can be found in [8]–[11]. Here, we provide only the basic idea.

To begin with, assume that all the objects of interest are elements of a Hilbert space $\mathcal{F}$. Now, consider a convex set $C \subset \mathcal{F}$; then, for any $\boldsymbol{x} \in \mathcal{F}$, the projection $P\boldsymbol{x}$ of $\boldsymbol{x}$ onto C is the element in C *closest* to $\boldsymbol{x}$. If C is closed and convex, $P\boldsymbol{x}$ exists and is uniquely determined by $\boldsymbol{x}$ and C from the minimality criterion

$$\|\boldsymbol{x} - P\boldsymbol{x}\| = \min_{\boldsymbol{g} \in C} \|\boldsymbol{x} - \boldsymbol{g}\|. \tag{6}$$

This rule, which assigns to every $\boldsymbol{x} \in \mathcal{F}$ its nearest neighbor in C, defines the (in general) nonlinear projection operator $P: \mathcal{F} \rightarrow C$ without ambiguity. In this paper, the norm operator $\|\cdot\|$ is taken to be the Euclidean norm. If $\boldsymbol{x}$ is already in C, then $P\boldsymbol{x} = \boldsymbol{x}$.

The basic idea of POCS is as follows: Every known property of the unknown $\boldsymbol{x} \in \mathcal{F}$ will restrict $\boldsymbol{x}$ to lie in a closed convex set C_i in $\mathcal{H}$. Thus, for m known properties, there are m closed convex sets $C_i, i = 1, 2, \cdots, m$ and $\boldsymbol{x} \in C_0 \triangleq \cap_{i=1}^{m} C_i$. Then, the problem is to find a point of C_0 given the sets C_i and projection operators P_i projecting onto $C_i, i = 1, 2, \cdots, m$. The set C_0 is sometimes called the *solution set* since any element of C_0 satisfies all the constraints and therefore represents a feasible solution. Often, but not always, it is clear whether a solution set C_0 exists or not. When C_0 is empty, the user must decide which constraint set can be enlarged at the lowest design cost. Based on fundamental theorems given by Opial [12] and Gubin *et al.* [5], the sequence $\{\boldsymbol{x}_k\}$ generated by the recursion relation

$$\boldsymbol{x}_{k+1} = P_m P_{m-1} \cdots P_1 \boldsymbol{x}_k, \qquad k = 0, 1, \cdots \tag{7}$$

converges weakly to a point C_0.

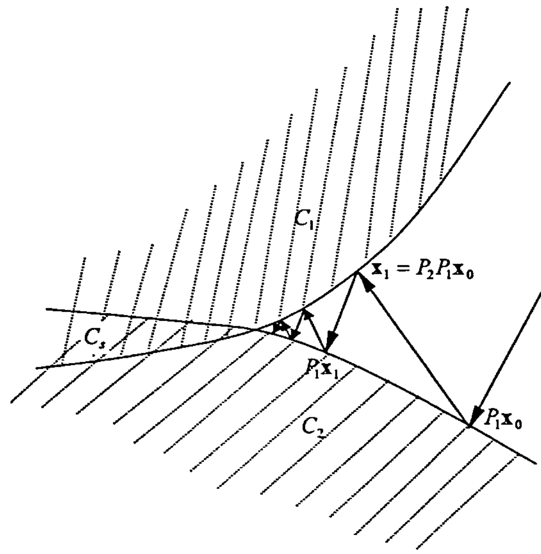

Fig. 2. Trajectory of iteration in POCS with two sets. The set C_s is the solution region, and x_0 is an arbitrary starting point.

There are generalizations of (7) that often can increase the rate of convergence. However, a discussion of these generalizations is tangential to the objective of this paper and, hence, will be omitted. For further details, see [7].

Fig. 2 shows a trajectory of the iterates $\boldsymbol{x}_k$ in an application of POCS when two convex constraint sets are involved.

IV. Design of Linear-Phase Crossover Filters Using VSPM

The first step in implementing the VSPM algorithm is to define the appropriate sets that capture the crossover analysis filters properties. These sets are parameterized by the constraints needed to specify the characteristics of the filters. Let us define

$$\mathcal{H} \in \prod^{M} \boldsymbol{R}^N, \quad \mathcal{G} \in \prod^{M} \boldsymbol{R}^N \quad \text{as} \quad \mathcal{H} \triangleq (\boldsymbol{h}_1, \boldsymbol{h}_2, \cdots, \boldsymbol{h}_M)$$

$$\mathcal{G} \triangleq (\boldsymbol{g}_1, \boldsymbol{g}_2, \cdots, \boldsymbol{g}_M), \quad \mathcal{H} \leftrightarrow \boldsymbol{H} \triangleq (H_1(\omega), \cdots, H_M(\omega))$$

$$\mathcal{G} \leftrightarrow \boldsymbol{G} \triangleq (G_1(\omega), \cdots, G_M(\omega))$$

$$S \triangleq \left|\sum_{i=1}^{M} G_i(\omega)\right| \quad \text{and} \quad S_m \triangleq \left|\sum_{\substack{i=1\\ i\neq m}}^{M} G_i(\omega)\right|$$

where $G_i(\omega) = |G_i| e^{j\varphi_i(\omega)}$ for $i = 1, 2, \cdots, M$, and $\mathcal{G}$ is an arbitrary M-tuple whose components are $\boldsymbol{g}_i, i = 1, \cdots, M$. In addition, "$\leftrightarrow$" indicates Fourier pairs. Ideally, the VSPM iterative algorithm should be implemented via the discrete-time Fourier transform, and therefore, N represents the size of the fast Fourier transform (FFT). $\boldsymbol{R}^N$ is the space of real vectors with N components, and $\boldsymbol{h}_i, i = 1, \cdots, M$ is the vector with the first L components representing the impulse response of the filter controlling the frequency response in the ith band. In parallel with (1) and taking into consideration the stopband attenuations, we define the following appropriate sets for an M-way crossover system. Best defined in the frequency domain, these sets are

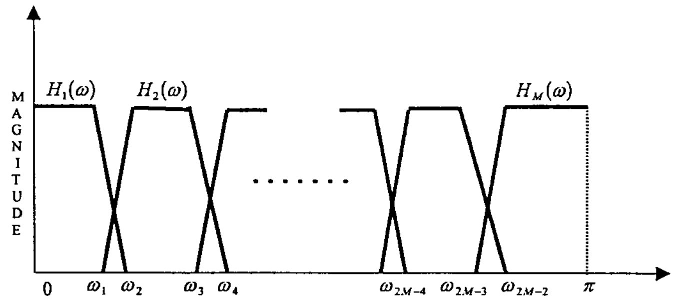

Fig. 3. Crossover filters magnitude response for a M-way system.

$$C_1' \triangleq \left\{ \mathcal{H}\colon a(\omega) \le \left|\sum_{i=1}^{M} H_i(\omega)\right| \le b(\omega) \quad \text{and} \right.$$
$$\arg[H_i(\omega)] = \varphi_i(\omega) = \omega(L-1)/2$$
$$\left. \text{for } 1 \le i \le M \quad \text{and for } \omega \in (0, \pi) \right\} \tag{8}$$

$$C_{2m} \triangleq \left\{ \mathcal{H}\colon \left|\sum_{\substack{i=1\\ i\neq m}}^{M} H_i(\omega)\right| \le \delta(\omega) \text{ for } \omega \in (\omega_{2m-2}, \omega_{2m-1}) \right\}$$
$$\text{for } m = 1, \cdots, M \tag{9}$$

$$C_{3m} \triangleq \left\{ \mathcal{H}\colon \left|\sum_{\substack{i=1\\ i\neq m, m+1}}^{M} H_i(\omega)\right| \le \delta(\omega) \text{ for } \omega \in (\omega_{2m-1}, \omega_{2m}) \right\}$$
$$\text{for } m = 1, \cdots, M-1 \tag{10}$$

where $\omega_i, i = 0, \cdots, 2M-1$ are the break frequencies as shown in Fig. 3. Note that $\omega_0 = 0$ and that $\omega_{2M-1} = \pi$. In addition to the above sets, we define the following linear-phase constraint set in the time domain:

$$C_4 \triangleq \left\{ \mathcal{H}\colon \left| \begin{array}{c} h_i(n) = h_i(L-n-1), \text{for } i = 1, \cdots, M \\ \text{and for } n = 0, 1, \cdots, L-1 \\ h_i(n) = 0, \text{for } i = 1, \cdots, M \text{ and for} \\ n = L, L+1, \cdots, N-1 \end{array} \right. \right\}. \tag{11}$$

In words, C_1' is the set of all M-tuple, finite-length, sequences that imply a Fourier transform that satisfies (1) with an error tolerance region of width $b(\omega) - a(\omega)$. The sets $C_{2m}, m = 1, \cdots, M$ are the sets that constrain the magnitude-summed frequency responses of all subband filters, except the mth, to a level of δ in the passband of the mth filter. The sets $C_{3m}, m = 1, \cdots, M-1$ are the sets of all M-tuple finite-length sequences with magnitude-summed stopband attenuation bounded by $delta$ for different transition bands in the spectrum. The set C_4 is the set of all symmetrical sequences $\boldsymbol{h}_i, i = 1, \cdots, M$ that satisfies the crossover filter's linear phase property and impulse response of length L. The convexity of C_1' is shown below. The convexity of the other sets can be established using similar arguments as for the sets defined in [7, pp. 225–228].

Convexity of C_1': Let $\mathcal{H}$ and $\mathcal{H}' \in C_1'$ and $\mu\mathcal{H} + (1-\mu)\mathcal{H}' \leftrightarrow (1-\mu)\boldsymbol{H}'$. Then, for $0 \le \mu \le 1$, define $\tilde{\boldsymbol{H}} \triangleq \mu\boldsymbol{H} +$

$(1-\mu)\boldsymbol{H}'$. However, $\mu\boldsymbol{H}+(1-\mu)\boldsymbol{H}' = \mu H_1(\omega)+(1-\mu)H_1'(\omega),\cdots,\mu H_M(\omega)+(1-\mu)H_M'(\omega)$. We must show that $a(\omega)\le|\Sigma_{i=1}^M \tilde{H}_i(\omega)|\le b(\omega)$. Since the phases of all elements are equal, the phase term can be factored out to yield

$$\begin{aligned}\left|\sum_{i=1}^M \tilde{H}_i(\omega)\right| &= \left|\sum_{i=1}^M \mu H_i(\omega)+(1-\mu)H_i'(\omega)\right|\\ &= \sum_{i=1}^M (\mu|H_i(\omega)|+(1-\mu)|H_i'(\omega)|). \qquad (12)\end{aligned}$$

The term on the right-hand side is bounded from above by $b(\omega)$ since $\mu b(\omega)+(1-\mu)b(\omega)=b(\omega)$ and from below by $a(\omega)$ since $\mu a(\omega)+(1-\mu)a(\omega)=a(\omega)$. Therefore, $\tilde{\boldsymbol{H}}\in C_1'$, and C_1' is convex.

The next step is to find the projections onto these sets. The projections are computed using the Lagrange multiplier method and worked out in the Appendix. In this section, we only furnish the results.

As pointed out in the Appendix, it is not necessary to compute the projections onto C_1' since all iterates are confined to the subspace of functions with linear phase as a result of projecting onto C_4. The other projections do not affect the phase. For this reason, we relax the constraints in C_1' by removing the linear phase constraint. The resulting set, which we call C_1, is the one that we deal with in what follows.

Projection onto C_1: The projection of an arbitrary M-tuple $\mathcal{G}$ onto C_1 is $\mathcal{H}^*=P_1\mathcal{G}\leftrightarrow\boldsymbol{H}^*$, where the components of $\boldsymbol{H}^*$ are

$$H_i^*(\omega)=\begin{cases}G_i(\omega)-\dfrac{1}{M}(S(\omega)-b(\omega))e^{\varphi(\omega)} & \text{if } S(\omega)>b(\omega)\\ G_i(\omega), & \text{if } a(\omega)\le S(\omega)\le b(\omega)\\ G_i(\omega)+\dfrac{1}{M}(a(\omega)-S(\omega))e^{\varphi(\omega)} & \text{if } S(\omega)<a(\omega).\end{cases} \qquad (13)$$

Projection onto $C_{2m}, m=1,\cdots,M$: The projection of an arbitrary M-tuple $\mathcal{G}$ onto C_{2m} is $\mathcal{H}^*=P_{2m}\mathcal{G}\leftrightarrow\boldsymbol{H}^*$, where the components of $\boldsymbol{H}^*$ are

$$H_i^*(\omega)=\begin{cases}G_i(\omega)-\dfrac{1}{M-1}(S_m(\omega)-\delta(\omega))e^{\varphi(\omega)} & \text{for } \omega\in(\omega_{2m-2},\omega_{2m-1}), i\ne m \text{ and } S_m(\omega)>\delta(\omega)\\ G_i(\omega), & \text{for } \omega\in(\omega_{2m-2},\omega_{2m-1}), i=m \text{ and } S_m(\omega)>\delta(\omega)\\ G_i(\omega), & \text{for } \omega\in(\omega_{2m-2},\omega_{2m-1}) \text{ and } S_m(\omega)\le\delta(\omega)\\ G_i(\omega), & \text{for } \omega\notin(\omega_{2m-2},\omega_{2m-1})\end{cases} \qquad (14)$$

Projection onto $C_{3m}, m=1,\cdots,M-1$: The projection of an arbitrary M-tuple $\mathcal{G}$ onto C_{3m} is $\mathcal{H}^*=P_{3m}\mathcal{G}\leftrightarrow\boldsymbol{H}^*$, where the components of $\boldsymbol{H}^*$ are

$$H_i^*(\omega)=\begin{cases}G_i(\omega)-\dfrac{1}{M-2}(S_{m,m+1}(\omega)-\delta(\omega))e^{\varphi(\omega)} & \text{for } \omega\in(\omega_{2m-1},\omega_{2m}), i\ne m,m+1 \text{ and } S_{m,m+1}(\omega)>\delta(\omega)\\ G_i(\omega), & \text{for } \omega\in(\omega_{2m-1},\omega_{2m}), i=m,m+1 \text{ and } S_{m,m+1}(\omega)>\delta(\omega)\\ G_i(\omega), & \text{for } \omega\in(\omega_{2m-1},\omega_{2m}) \text{ and } S_{m,m+1}(\omega)\le\delta(\omega)\\ G_i(\omega), & \text{for } \omega\notin(\omega_{2m-1},\omega_{2m})\end{cases} \qquad (15)$$

Projection onto C_4: The projection of an arbitrary M-tuple onto C_4 is $\mathcal{H}^*=P_4\mathcal{G}$, where

$$h_i^*(n)=\begin{cases}\dfrac{g_i(n)+g_i(L-n-1)}{2} & \text{for } i=1,\cdots,M \text{ and for } n=0,1,\cdots,L-1\\ 0, & \text{for } i=1,\cdots,M \text{ and for } n=L,L+1,\cdots,N-1.\end{cases} \qquad (16)$$

With the exception of set C_4, the projection onto all other sets are conveniently done in the frequency domain. Observe that each of the sets $C_1, C_{2m}, m=1,\cdots,M, C_{3m}, m=1,\cdots,M-1$ depends on the continuous frequency variable ω. Since the projections onto these sets are realized numerically, the frequency range $(0,\pi)$ is partitioned onto a grid of discrete-frequency values commensurate with the of size N with $\Delta\triangleq 2\pi/(N-1)$. The discrete frequencies are given by $\omega_n=n\Delta, n=0,2,\cdots,N-1$. Now, consider a frequency plane projector such as P_1; this projector furnishes a correction at every frequency ω_n $n=0,1,\cdots,N/2$ (due to the symmetry of $G_i(\omega)$ around π $i=1,\cdots,M$ projections need to be performed only from 0 to π, which only cuts the computations in half). If $P_1(\omega_n)$ denotes the application of projector P_1 at ω_n, then the full action P_1 can be described by the composition of single-frequency operators $P_1(\omega_0)P_1(\omega_1)\cdots P_1(\omega_{N/2})$ or

$$P_1=\prod_{n=0}^{N/2} P_1(\omega_n) \qquad (17)$$

where $\omega_{N/2}=\pi$. It is the same with projectors $P_{2m}, m=1,\cdots,M$ and $P_{3m}, m=1,\cdots,M-1$; each of these can be represented by a composition of single-frequency operators.

The projector P_4, which projects onto C_4, depends on the discrete-time variable n. If we denote $P_4(n)$ as the application of P_4 at specific time n, then the overall action of P_4 can be written as a composition of specific-time operators $P_4(n)$ $n=0,1,\cdots,N-1$, i.e.,

$$P_4=\prod_{n=0}^{N-1} P_4(n). \qquad (18)$$

For the special but important case $M=3$, the VSPM algorithm takes the form

$$\mathcal{G}_{k+1}=P_1P_{21}P_{22}P_{23}P_{31}P_{32}P_4\mathcal{G}_k \;\; \mathcal{G}_0 \text{ arbitrary} \qquad (19)$$

where projectors $P_1, P_{21}, P_{22}, P_{23}, P_{31}, P_{32}$ are compositions of the form shown in (17). Each projection is called a step. A new iteration cycle begins after seven steps.

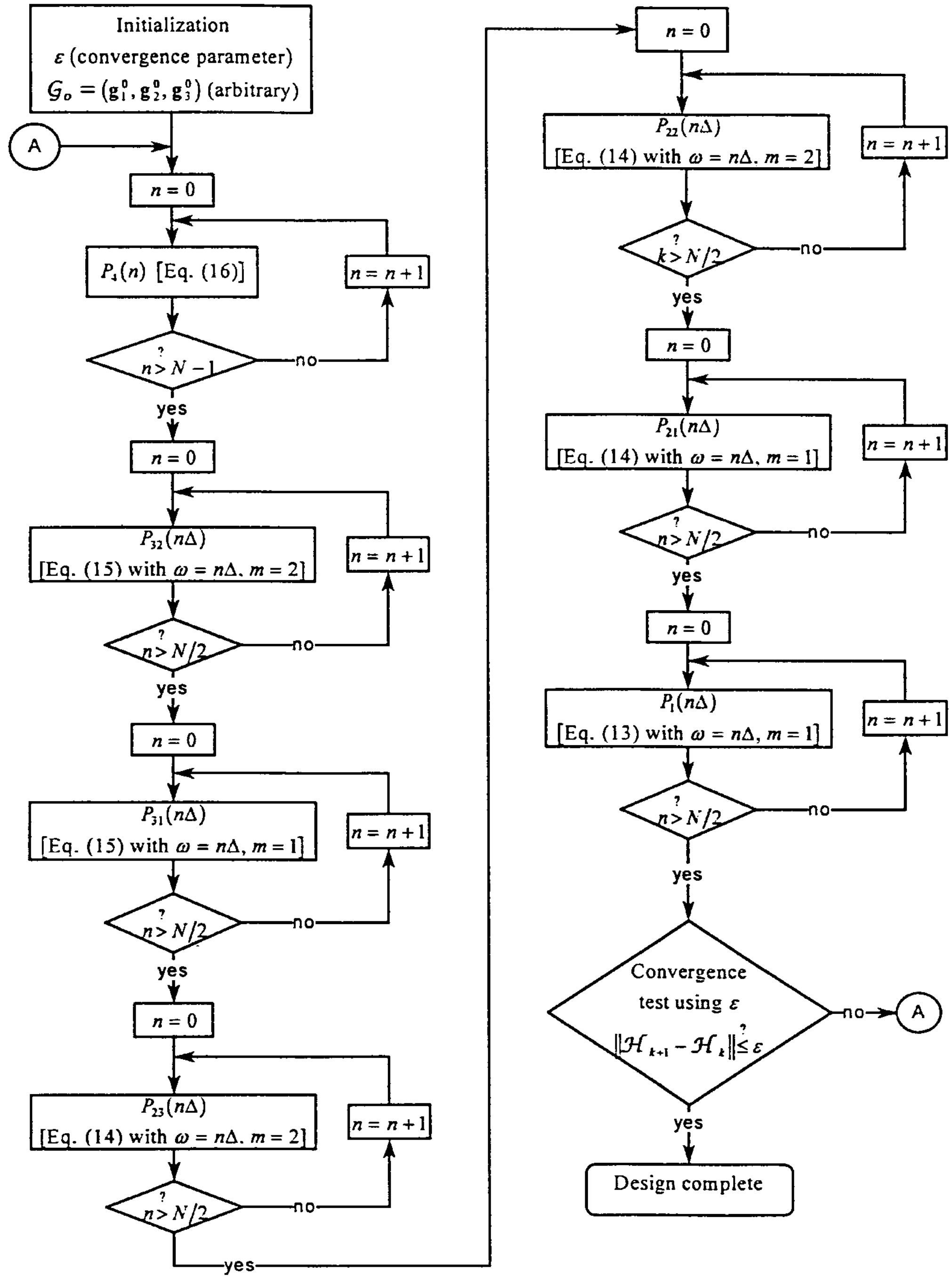

Fig. 4. Flowchart showing the numerical realization of (19).

Fig. 4 is a flowchart of the algorithm for $M = 3$, i.e., three crossover filters. Compositions of the projectors are realized by loops. In practice, there is much room for optimization of the algorithm, which we do not show for simplicity. For example, projecting onto C_{21} requires modification of $G_i(\omega)$ $i = 1, 2, 3$ only over the band $(0, \omega_1)$. Likewise, projecting onto C_{22} involves modification of $G_i(\omega)$ $i = 1, 2, 3$ only over the band (ω_2, ω_3), etc., for the others.

V. Examples and Numerical Results

In both of the following two examples, we chose $N = 512$. The iterative procedure stops when $\|\boldsymbol{h}_i^{k+1} - \boldsymbol{h}_i^k\| < \epsilon$ for $i = 1, 2, 3$. In our design examples, we used $\epsilon = 10^{-6}$. The crossover systems designed are for a three-way system, i.e., $M = 3$ in (1). In the first example, we assume that the loudspeaker has a flat SPL over the entire audio spectrum and does not need to be equalized. The crossover system is designed for spectrum splitting only. The normalized critical frequencies in both examples are chosen realistically to accommodate a three-way system to be $\omega_1 = 0.12\pi, \omega_2 = 0.2\pi, \omega_3 = 0.4\pi$, and $\omega_4 = 0.48\pi$.

In the second example, we hypothetically model the SPL of the loudspeaker as $L(\omega) = 1 + 0.15\ \cos(0.035\omega), 0 \le \omega \le \pi$; see the top part of Fig. 8. The crossover system is designed for spectrum splitting as well as to equalize the SPL.

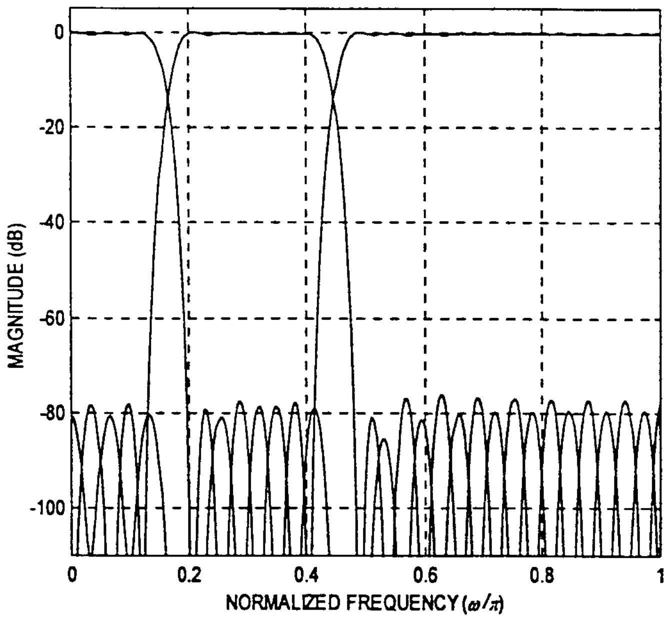

Fig. 5. Frequency response for the crossover system for a three-way system.

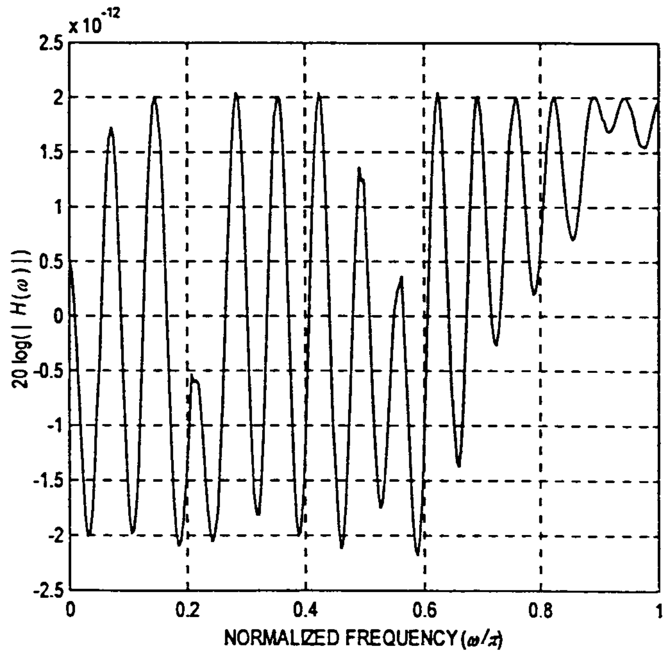

Fig. 6. Plot of $H(\omega)$.

Choice of the Design Parameters: A practical way to design the crossover filters is that we start by specifying the values $\delta(\omega), a(\omega)$, and $b(\omega)$ for an acceptable deviation for a given application and then look for the minimum filter order L realizing these specification (i.e., so that the intersection of all the constraint sets is not empty). Following this procedure, we can easily pick the required filter order over a few runs of the presented algorithm. The number of iteration cycles needed to reach convergence decreases significantly when increasing the size of the intersection set.

Example 1—Design Of Crossover Filter for Spectrum Splitting

In this example, a linear-phase crossover system was designed with length $L = 65, a(\omega) = 1 - 10^{-12}, b(\omega) = 1 + 10^{-12}, \delta(\omega) = 0.024$. For the above values of $L, \delta(\omega), a(\omega)$, and $b(\omega)$, the intersection of all the constraint sets is not empty. Fig. 5 shows the frequency response, and Fig. 6 shows the plot of $H(\omega)$. The peak-to-peak deviation is negligible, and this leads to a near-perfect reconstruction, i.e., errors of 10^{-12} the order of of the input signal. Thus, we may write

$$x(n-(L-1)/2) = \sum_{i=1}^{3} \sum_{k=-\infty}^{\infty} x(k)h_i(n-k). \tag{20}$$

The proposed algorithm for this example converged after some 10 000 iteration cycles (3 min on a 300-MHz Pentium PC using MATLAB).

Example 2—Design of Crossover System for Spectrum Splitting and Equalization

In this example, a linear-phase crossover system was designed with length $L = 65, a(\omega) = (1/L(\omega)) - 0.0023, b(\omega) = (1/L(\omega)) + 0.0023, \delta(\omega) = 0.024$. For these values of $L, \delta(\omega), a(\omega)$, and $b(\omega)$, there is a nonempty intersection of all the constraints sets. Fig. 7 shows the frequency response, and Fig. 8 shows the plots of $L(\omega)$ (top), $H(\omega)$ (middle), and of $L(\omega)H(\omega)$ (bottom). The peak-to-peak deviation of $L(\omega)H(\omega)$ as a result of equalization is small (about 0.1 dB). The proposed algorithm for this example converged after about 23 000 iteration cycles (7 min on a 300-MHz Pentium PC using MATLAB).

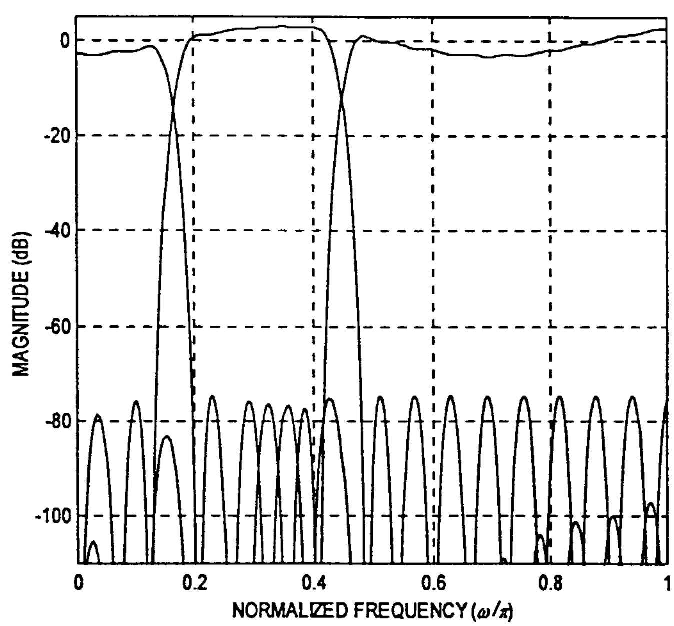

Fig. 7. Frequency response for the crossover system for a three-way system.

VI. Concluding Remarks

In this paper, a new and promising vector-space design method for an important class of digital, linear-phase, FIR filters was presented. The method has significant flexibility in that any number of constraints can be incorporated in the

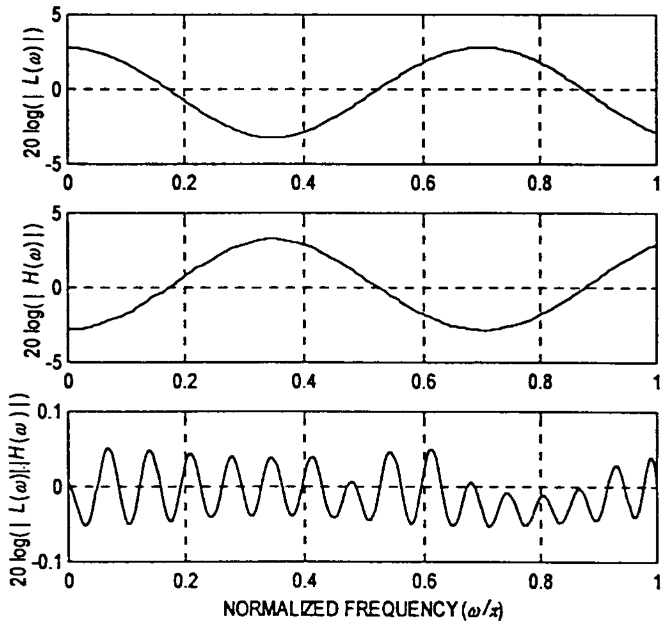

Fig. 8. Plot of the speaker SPL (upper), $H(\omega)$ (middle), and $H(\omega)L(\omega)$ (lower), in decibels.

design without the need to find one-step analytical solutions. In addition, vector space projections allow the design of arbitrary M-way crossover systems as easily as a three-way system.

APPENDIX

Projection onto C_1: Finding the projection of an arbitrary $(\boldsymbol{g}_1, \cdots, \boldsymbol{g}_M) \leftrightarrow (G_1, \cdots, G_M) \triangleq \boldsymbol{G}$ onto C_1 involves finding the *infinum* (minimum) over all $(\boldsymbol{h}_1, \cdots, \boldsymbol{h}_M) \leftrightarrow (H_1, \cdots, H_M) \triangleq \boldsymbol{H}$ in C_1 of the Lagrange functional

$$\begin{aligned} J(\boldsymbol{H}, \lambda) = \sum_{i=1}^{M} |H_i(\omega) - G_i(\omega)|^2 + \lambda_0 \left(\left| \sum_{i=1}^{M} H_i(\omega) \right| - \xi(\omega) \right) \\ + \sum_{i=1}^{M} \lambda_i \left(\frac{H_{Ri}(\omega)}{|H_i(\omega)|} - \cos\left(\frac{L-1}{2}\right)\omega \right) \end{aligned} \tag{21}$$

where $H_{Ri}(\omega)$ is the real component of $H_i(\omega)$, the first term on the right-hand side measures the distance from $\boldsymbol{G}$ to $\boldsymbol{H}$, the second term is the imposition of the magnitude tolerance constraints, and the third term ensures that all the filters have phase $\varphi(\omega) = \omega(L-1)/2$. Note that $\xi(\omega)$ is assigned the value $\xi(\omega) \triangleq b(\omega)$ if $|\Sigma_{i=}^{M} G_i(\omega)| \geq b(\omega)$, and $\xi(\omega) \triangleq a(\omega)$ if $|\Sigma_{i=1}^{M} G_i(\omega)| \leq a(\omega)$.

The solution of (21) involves finding $M+1$ constraints $\lambda_0, \lambda_1, \cdots, \lambda_M$ in addition to finding the projection variables $H_i^*(\omega), i = 1, \cdots, M$. While this is possible, *it is not necessary,* the reason being that every iteration involves elements only from the subspace of functions with linear phase, where the last is a consequence of projecting onto C_4. The constraints in C_4 imply the well-known linear-phase constraint. Hence, every element $(\boldsymbol{g}_1, \cdots, \boldsymbol{g}_M) \leftrightarrow \boldsymbol{G}$ will have the form

$$\boldsymbol{G} = (|G_1(\omega)|e^{j\varphi(\omega)}, \cdots, |G_M(\omega)|e^{j\varphi(\omega)}). \tag{22}$$

This allows the computation of the projection to be much easier since the third term on the right-hand side of (21) (i.e., the linear phase constraints) can be eliminated. For the sake of brevity, we have already applied this simplifying assumption in the definition of C_{2m} and C_{3m}.

Assuming that all elements are confined to the subspace of functions of linear phase $\varphi(\omega)$, to compute the projection of an arbitrary M-tuple $\boldsymbol{G}$ onto C_1, we write the Lagrange functional as

$$J(\boldsymbol{H}, \lambda) = \sum_{i=1}^{M} |H_i - G_i|^2 + \lambda \left(\left| \sum_{i=1}^{M} H_i \right| - \xi \right) \tag{23}$$

where, for simplicity of notation, $H_i = H_i(\omega), G_i = G_i(\omega), \xi = \xi(\omega), a = a(\omega)$, and $b = b(\omega)$. We note that since

$$\begin{aligned} H_i &= |H_i| e^{j\varphi} \\ \left| \sum_{i=1}^{M} H_i \right| &= \left| \sum_{i=1}^{M} |H_i| e^{j\varphi} \right| = \left| e^{j\varphi} \sum_{i=1}^{M} |H_i| \right| = \sum_{i=1}^{M} |H_i|. \end{aligned}$$

Let $H_i \triangleq \Delta H_{Ri} + jH_{Ii}$ and $G_i \triangleq G_{Ri} + jG_{Ii}$, where the subscript prefixes R and I stand for "real" and "imaginary," respectively. Thus, (23) is rewritten as

$$\begin{aligned} J(\boldsymbol{H}, \lambda) = \sum_{i=1}^{M} ((H_{Ri} - G_{Ri})^2 + (H_{Ii} - G_{Ii})^2) \\ + \lambda \left(\sum_{i=1}^{M} (H_{Ri}^2 + H_{Ii}^2)^{1/2} - \xi \right) \end{aligned} \tag{24}$$

and computing $\partial J / \partial H_{Rk} - \partial J / \partial H_{Ik} = 0$ yields

$$(H_{Rk} - G_{Rk}) + \frac{\lambda}{2}(H_{Rk}^2 + H_{Ik}^2)^{-(1/2)} H_{Rk} = 0 \tag{25}$$

$$(H_{Ik} - G_{Ik}) + \frac{\lambda}{2}(H_{Rk}^2 + H_{Ik}^2)^{-(1/2)} H_{Ik} = 0. \tag{26}$$

Multiplying (26) by $j = \sqrt{-1}$ and adding (25) and (26) yields

$$H_k = G_k - \frac{\lambda}{2} e^{j\varphi} \tag{27}$$

where we see that $H_k / |H_k| = e^{j\varphi}$.

To find λ, we consider the three cases $|\Sigma_{i=1}^{M} G_i| > b, |\Sigma_{i=1}^{M} G_i| < a$, and $a \leq |\Sigma_{i=1}^{M} G_i| \leq b$.

Case 1: $|\Sigma_{i=1}^{M} G_i| > b$. For this case, the projection of $\boldsymbol{G}$ will lie on the upper boundary of C_1, and hence, the projection will satisfy

$$\left| \sum_{i=1}^{M} H_i \right| = b. \tag{28}$$

Then, from (27) and (28), we get

$$\left| \sum_{k=1}^{M} \left(G_k - \frac{\lambda}{2} e^{j\varphi} \right) \right| = b \tag{29}$$

or, since $G_k = |G_k| e^{j\varphi}$

$$\left| \sum_{k=1}^{M} \left(|G_k| - \frac{\lambda}{2} \right) \right| = b. \tag{30}$$

Define $S \triangleq \Sigma_{i=1}^{M} |G_k| > 0$. Then, from (30) $b^2 = (S - M\lambda/2)^2$ or, equivalently

$$\left(\frac{\lambda}{2}\right)^2 - 2\left(\frac{S}{M}\right)\frac{\lambda}{2} + \frac{S^2 - b^2}{M^2} = 0 \tag{31}$$

which yields the two roots

$$r_1 \triangleq \left(\frac{\lambda}{2}\right)_1 = \frac{S-b}{M} \quad \text{and} \quad r_2 \triangleq \left(\frac{\lambda}{2}\right)_2 = \frac{S+b}{M}. \tag{32}$$

The first root yields the solution

$$H_k = G_k - \frac{1}{M}(S-b)e^{j\varphi} \tag{33}$$

whereas the second root yields

$$H_k = G_k - \frac{1}{M}\,(S+b)e^{j\varphi}. \tag{34}$$

The solution for H_k in (33) and (34) both satisfy the set membership constraints i.e.,

$$\left|\sum_{k=1}^{M} H_k\right| = b \quad \text{and} \quad \arg[H_k] = \varphi \tag{35}$$

and, hence, are elements of points in C_1. However, for root r_1, the distance from G to H is $\|\boldsymbol{G}-\boldsymbol{H}\| = S-b$, whereas for root r_2, it is $\|\boldsymbol{G}-\boldsymbol{H}\| = S+b$. Hence, only $r_1 = (S-b)/M$ yields the correct projection, which is (33) repeated as

$$H_k = G_k - \frac{1}{M}(S-b)e^{j\varphi} \qquad k = 1, \cdots, M. \tag{36}$$

Case 2: $|\Sigma_{i=1}^{M} G_i| < a$. For this case, the projection of $\boldsymbol{G}$ will lie on the lower boundary of C_1 and, hence, the projection will satisfy $|\Sigma_{i=1}^{M} H_i| = a$. Proceeding exactly as in Case 1, we obtain

$$H_k = G_k + \frac{1}{M}(a-S)e^{j\varphi} \qquad k = 1, \cdots, M. \tag{37}$$

Case 3: $a \le |\Sigma_{i=1}^{M} G_i| \le b$. For this case, no correction is needed since $\boldsymbol{G}$ is already in the set.

Projection onto C_{2m}: The Lagrange functional for this case is

$$J(\boldsymbol{H}, \lambda) = \sum_{i=1}^{M} |H_i - G_i|^2 + \lambda\left(\left|\sum_{\substack{i=1\\ i\neq m}}^{M} H_i\right| - \delta\right). \tag{38}$$

Proceeding exactly as when we computed the projection onto C_1, we obtain for $\omega \in (\omega_{2m-2}, \omega_{2m-1})$

$$\begin{aligned} H_k^* &= G_k - \frac{\lambda}{2}\,e^{j\varphi} \qquad k \neq m \\ H_k^* &= G_k \qquad k = m. \end{aligned} \tag{39}$$

Using the constraints that

$$\left|\sum_{\substack{i=1\\ i\neq m}}^{M} H_i\right| = \delta \text{ when } \left|\sum_{\substack{i=1\\ i\neq m}}^{M} G_i\right| > S$$

we obtain, as the projection

$$\begin{aligned} H_k^* &= G_k - \frac{S_m - \delta}{M-1}\,e^{j\varphi} \qquad k \neq m \\ H_k^* &= G_k \qquad k = m \end{aligned} \tag{40}$$

where

$$S_m \triangleq \left|\sum_{\substack{i=1\\ i\neq m}}^{M} G_i\right|.$$

When $S_m \le \delta$ or $\omega \notin (\omega_{2m-2}, \omega_{2m-1})$, then $\boldsymbol{H}^* = \boldsymbol{G}$ since $\boldsymbol{G}$ is already in the set.

Projection onto C_{3m}: Following the method of the previous two computations, we can write, by inspection for $\omega \in (\omega_{2m-1}, \omega_{2m})$

$$\begin{aligned} H_k^* &= G_k - \frac{S_{m,m_1} - \delta}{M-2}e^{j\varphi} \qquad k \neq m, m+1 \\ H_k^* &= G_k \qquad k = m, m+1 \end{aligned} \tag{41}$$

where

$$S_{m,m+1} \triangleq \left|\sum_{\substack{i=1\\ i\neq m,m+1}}^{M} G_i\right|.$$

When $S_{m,m+1} \le \delta$ or $\omega \notin (\omega_{2m-1}, \omega_{2m})$, then $\boldsymbol{H}^* = \boldsymbol{G}$ since $\boldsymbol{G}$ is already in the set.

Projection onto C_4: The Lagrange functional for this case is

$$\begin{aligned} J(\mathcal{H}, \lambda) = \sum_{m=0}^{(L-1)/2} \sum_{i=1}^{M} &((h_i(m) - g_i(m))^2 \\ &+ \lambda_i(h_i(m) - h_i(L-m-1))). \end{aligned}$$

We solve for $\boldsymbol{h}_i^*$ for $i = 1, \cdots, M$ by setting for $n = 0, 1, \cdots, (L-1)/2$: $\partial J/\partial h_i(m)|_{m=n} = \partial J/\partial h_i(L-m-1)|_{m=n} = 0$, and using the equations $h_i(n) = h_i(L-n-1)$, we get

$$h_i^*(n) = \frac{g_i(n) + g_i(L-n-1)}{2} \quad \text{for } i = 1, 2, \cdots, M. \tag{42}$$

References

[1] P. Garde, "All-pass crossover systems," *J. Audio Eng. Soc.*, vol. 34, no. 11, p. 889, 1986.

[2] P. S. Lipshitz and J. Vanderkooy, "In-phase crossover network design," *J. Audio Eng. Soc.*, vol. 28, no. 9, p. 575, 1980.

[3] F. Mintzer, "On half-band, third-band and Nth band FIR filters and their design," *IEEE Trans. Acoust., Speech, Signal Processing*, vol. ASSP-30, pp. 734–738, Oct. 1982.

[4] L. M. Bregman, "Finding the common point of convex sets by the method of successive projections," *Dokl. Akad. Nauk. USSR*, vol. 162, no. 3, p. 487, 1965.

[5] L. G. Gubin, B. T. Polyak, and E. V. Raik, "The method of projections for finding the common point of convex sets," *USSR Comput. Math. Phys.*, vol. 7, no. 6, p. 1, 1967.

[6] D. C. Youla and H. Webb, "Image reconstruction by the method of projections onto convex sets—Part I," *IEEE Trans. Med. Imag.*, vol. M1-1, p. 95, 1982.

[7] H. Stark and Y. Yang, *Vector space projection methods: A Numerical Approach to Signal and Image Processing, Neural Nets and Optics*. New York: Wiley, 1998.

[8] D. C. Youla, "Mathematical theory of image restoration by the method of convex projections," in *Image Recovery: Theory and Applications*, H. Stark, Ed. Orlando, FL: Academic, 1987, ch. 2.

[9] H. Stark and M. I Sezan, "Image processing using projections methods," in *Real-Time Optical Information Processing*, J. Horner and B. Javidi, Eds. Orlando, FL: Academic, 1994, pp. 185–232.

[10] M. I. Sezan, "An overview of convex projections theory and its applications to image recovery problems," *Ultramicroscopy*, vol. 40, no. 1, pp. 55–67, 1992.

[11] K. C. Haddad, H. Stark, and N. P. Galatsanos, "Design of two-channel equiripple FIR linear-phase quadrature mirror filters using the vector space projection method," *IEEE Signal Processing Lett.*, vol. 5, July 1998.

[12] Z. Opial, "A Weak convergence of the sequence of successive approximation for nonexpansive mappings," *Bull. Amer. Math. Soc.*, vol. 73, p. 591, 1967.

Khalil C. Haddad was born in Beirut, Lebanon. He received the B.E. degree from American University of Beirut, the M.Sc. degree from the Florida Institute of Technology, Melbourne, and the Ph.D. degree from Illinois Institute of Technology, Chicago, in 1984, 1988, and 1998 respectively, all in electrical engineering. During his Ph.D. studies, he worked in industry.

Since 1999, he has been with Lucent Technologies, Holmdel, NJ. His main research interests are in digital signal processing and digital communication.

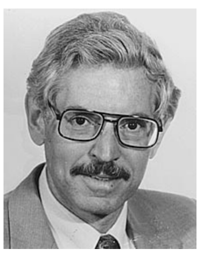

Henry Stark (F'88) received the B.S.E.E. degree from the City College of New York, New York, NY, in 1961 and the M.S.E.E. and Ph.D. degrees from Columbia University, New York, NY, in 1964 and 1968, respectively.

After working in industry for the Bendix Corporation and the Columbia University Electronics Research Labs, he spent 1969 and 1970 abroad at the Israel Institute of Technology, Haifa, and the Weizman Institute of Science. From 1970 to 1977, he was with the Department of Engineering and Applied Science, Yale University, New Haven, CT, and from 1977 to 1988, he was with the Department of Electrical and Computer Engineering, Rensselaer Polytechnic Institute, Troy, NY. He now holds the Carl and Paul Bodine Distinguished Professorship at Illinois Institute of Technology, Chicago, where he had been Chair of the Electrical and Computer Engineering Department from 1988 to 1997. He is the co-author (with J. W. Woods) of *Probability, Random Processes, and Estimation Theory for Engineers* (Englewood Cliffs, NJ: Prentice-Hall, 1986, 1994), *Modern Electrical Communications* (with F. B. Tuteur and J. B. Anderson, Englewood Cliffs, NJ: Prentice-Hall, 1979, 1988), and *Vector Space Projection Methods* (with Y. Yang, New York: Wiley, 1998). He has edited books on Fourier optics (*Applications of Optical Fourier Transforms*, New York: Academic, 1981) and image processing (*Image Recovery*, New York: Academic, 1987). He was written numerous papers, book chapters, and invited articles on signal processing, optics, medical imaging, and communications.

Dr. Stark was awarded a Best Paper Award by the IEEE Engineering in Medicine and Biology Society for a paper he co-authored with J. W. Woods, I. Paul, and R. Hingorani describing fast tomography. He is a Fellow of the Optical Society of America.

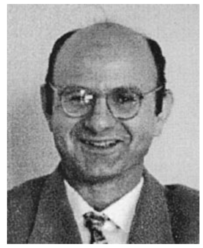

Nikolas P. Galatsanos (SM'95) received the Diploma of Electrical Engineering from the National Technical University of Athens, Athens, Greece, in 1982. He then received the M.S.E.E. and Ph.D. degrees from the Electrical and Computer Engineering Department, University of Wisconsin, Madison, in 1984 and 1989, respectively.

Since the fall of 1989, he has been on the faculty of the Electrical and Computer Engineering Department, Illinois Institute of Technology, Chicago, where currently, he is an Associate Professor. His research interests include inverse problems for visual communication and medical imaging applications and the application of vector space projection methods to signal and image processing problems.

Dr. Galatsanos has served as an Associate Editor for the IEEE TRANSACTIONS ON IMAGE PROCESSING and currently serves as an Associate Editor for the IEEE SIGNAL PROCESSING MAGAZINE. He has coedited, with A. K. Katsaggelos, a book entitled *Image Recovery Techniques for Image and Video Compression and Transmission* (Boston, MA: Kluwer, October 1998).